On the hydraulic behaviour of ITER Shield Blocks #14 and #08. Computational analysis and comparison with experimental tests

P.A. Di Maio[a], M. Merola[b], R. Mitteau[b], R. Raffray[b], E. Vallone[a,*]

[a] *Dipartimento di Energia, Ingegneria dell'Informazione e Modelli Matematici, Università di Palermo Viale delle Scienze, 90128, Palermo, Italy*
[b] *ITER Organization, Route de Vinon sur Verdon, 13067 Saint Paul Lez Durance, France*

As a consequence of its position and functions, the ITER blanket system will be subjected to significant heat loads under nominal reference conditions. Therefore, the design of its cooling system is particularly demanding. Coolant water is distributed individually to the 440 blanket modules (BMs) through manifold piping, which makes it a highly parallelized system. The mass flow rate distribution is finely tuned to meet all operation constraints: adequate margin to burn out in the plasma facing components, even distribution of water flow among the so-called plasma-facing "fingers" of the Blanket First Wall panels, high enough water flow rate to avoid excessive water temperature in the outlet pipes, maximum allowable water velocity lower than 7 m/s in manifold pipes. Furthermore the overall pressure drop and flow rate in each BM shall be within the fixed specified design limit to avoid an unduly unbalance of cooling among the 440 modules.

Analyses have to be carried out following a computational fluid-dynamic (CFD) approach based on the finite volume method and adopting a CFD commercial code to assess the thermal -hydraulic behaviour of each single circuit of the ITER blanket cooling system.

This paper describes the code benchmarking needed to determine the best method to get reliable and timely results. Since experimental tests are available in ITER Organization on full scale prototypes of Shield Blocks #08 and #14, CFD analyses have been performed to investigate their fluid-dynamic behaviour under steady state conditions and compare the numerical and experimental results. Results obtained are presented and critically discussed.

Keywords: Blanket, CFD analysis, hydraulics.

1. Introduction

The blanket system represents one of the pivotal components of the ITER reactor (Nuclear Facility INB-174), providing a physical boundary to the plasma and contributing to the thermal and nuclear shielding of the vacuum vessel, the superconducting magnets and the external ITER components. It is composed of 440 modules distributed in 18 toroidal sectors, covering a plasma-facing surface of ~650 m^2 [1].

From the structural standpoint, a typical blanket module is ~1 m high in poloidal direction, ~1.5 m long in toroidal direction and ~0.5 m thick in radial direction. It is composed of a plasma-facing First Wall (FW) panel and a Shield Block (SB), both actively cooled by pressurized water fed by a system of inlet/outlet manifolds connected to the Integrated Blanket, Edge-Localized Mode Coils and Divertor (IBED) Primary Heat Transfer System (PHTS) of the ITER Tokamak Cooling Water System (TCWS) [2].

As a consequence of its position and functions, the blanket system will be subjected to significant heat loads under nominal reference conditions, and the design of its cooling system is particularly demanding. In fact, it has to ensure that adequate cooling is provided to each module to promote convective heat transfer and to prevent burn out in its plasma facing components while complying with ITER pressure drop and flow velocity limits to avoid an unacceptably high pumping power and minimise corrosion concerns.

The Department of Energy, Information Engineering and Mathematical Models (DEIM) of the University of Palermo has collaborated with the ITER Organization (IO) on the assessment of the ITER blanket cooling system hydraulic performances under both steady state and draining and drying transient operational conditions [2-3].

A theoretical-computational research campaign has been launched following a computational fluid-dynamic (CFD) approach based on the finite volume method and adopting a qualified CFD commercial code to assess the steady state thermal-hydraulic behaviour of selected cooling circuits of the ITER blanket cooling system.

In particular, a code benchmarking activity has been carried out to determine the best method to get reliable and timely results, focusing the attention on the numerical assessment of the steady state hydraulic performances of the cooling circuits of Shield Blocks #08 and #14, for which experimental results of full scale prototype tested by the Korean and Chinese ITER Domestic Agencies, are available. This would then allow a direct comparison between numerical and experimental results.

This paper summarizes the code benchmarking activity, describing the discretization and modelling strategies adopted and critically comparing the numerical and experimental results obtained for the SBs #08 and #14 cooling circuits steady state fluid-dynamic behaviour.

author's email: eug.vallone@gmail.com

2. ITER blanket cooling system

The ITER blanket cooling system protects the blanket structure against overheating and extracts the nuclear deposited heat power. It relies on the use of sub-cooled water at inlet temperature and pressure of 70°C and 4.0 MPa, respectively, and is mainly composed of the following components [1]:

- SBs cooling circuits;
- FWs panels cooling circuits;
- hydraulic connectors;
- blanket manifolds system.

These components are arranged in 363 different cooling circuits, connected in parallel up to the TCWS Upper Ring Manifold and providing cooling water to the 440 separate modules of the ITER blanket. Most circuits individually cool a single blanket module, while some cool two modules in parallel and a few three modules in parallel, in order to comply with space constraints [4].

Each circuit is fed with a proper mass flow rate of water coolant (typically ranging from 4.7 kg/s to 9.6 kg/s for each blanket module), that enters from the inlet manifold being first routed to the inlet flexible pipe and, then, to the FW cooling circuit, from which it passes, through the outlet flexible pipe, to the SB cooling circuit. After circulating through the SB cooling channels, the coolant is finally routed into the outlet manifold, from which it is delivered back to the TCWS Upper Ring Manifold.

3. Hydraulic research campaign

As consequence of its architecture, the blanket cooling system is a highly parallelized network of 363 circuits, whose mass flow rates have to be properly tuned in order to guarantee the safe extraction of the 736 MW of thermal power under reference nominal conditions, while complying with operation constraints and requirements.

Therefore, a theoretical-computational research campaign has been launched by IO to assess coolant mass flow rate distribution inside each blanket cooling circuit so to check whether a well-balanced cooling would be ensured among the modules, fulfilling IO cooling system requirements in term of pressure drop, temperature increase, flow velocity and margin against critical heat flux occurrence.

A CFD approach based on the finite volume method has been adopted to carry out the research campaign and a suitable release of the ANSYS-CFX CFD code [1] has been selected as the reference computational tool. It is a well-known and qualified CFD commercial code intended to simulate in a fully 3D approach the thermofluid-dynamic behaviour of fluid flows. In particular, it numerically solves the fluid flow equations by adopting an element-based finite volume method, particularly suitable for analysing the thermofluid-dynamic behaviour of single-phase, single-component flows both in laminar and fully turbulent regimes.

A preliminary research activity has been carried out in close cooperation between DEIM and IO to assess clear guidelines for the CFD analyses in order to obtain reliable computational results within viable calculation times as well as to check the predictive potential of the ANSYS-CFX code for fusion-relevant applications. In particular, attention has been focussed on the CFD analysis of the steady state hydraulic behaviour of Shield Blocks #08 and #14, whose full-scale prototypes (FSP) have been already experimentally tested allowing for a reliable benchmarking of the ANSYS-CFX code.

3.1 Experimental tests

FSP of SBs #08 and #14 (Fig. 1) have been commissioned by IO and manufactured by the Korean and Chinese ITER Domestic Agencies, respectively. Thereafter, they have undergone experimental tests to investigate their steady-state hydraulic behaviour by assessing their hydraulic characteristic functions, $\Delta p=\Delta p(G)$, and in particular the pressure drop across the component, Δp, as a function of the corresponding mass flow rate, G, under steady state conditions [6].

(a)

(b)

Fig. 1. SB #08 (a) and SB #14 (b) test facilities.

3.2 Numerical analyses

A set of CFD parametric analyses has been performed for each SB cooling circuit investigated, to assess the pressure drop, Δp_i, needed to let each tested mass flow rate, G_i, flow through the circuit. The (G_i, Δp_i) pairs numerically assessed have been best fitted with a power-law analytical form and they have been compared to the experimental ones, allowing code benchmarking.

3.3 Finite volume models

Two 3D finite volume models have been properly set-up to realistically reproduce the geometric and flow features of SBs #08 and #14 flow domains (Figs. 2-3). Inlet and outlet sections have been chosen according to the technical specifications of DAs hydraulic tests.

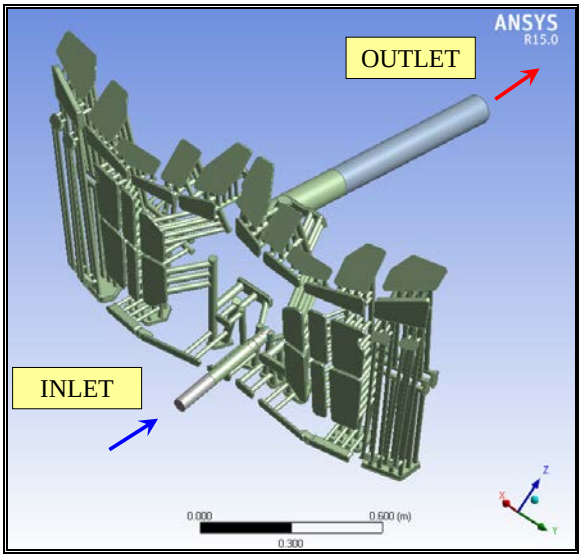

Fig. 2. SB#08 geometrical model.

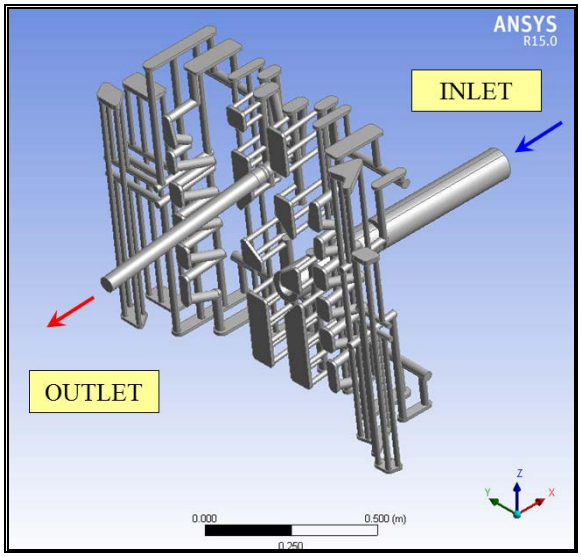

Fig. 3. SB#14 geometrical model.

3.3.1 Flow domain discretization

Proper sensitivity analyses have been carried out on mesh dimension to find the best compromise between accuracy and time consumption. It has been observed that generating models endowed with 1-3·10^6 nodes, for a common characteristic element length of 600 μm, provides numerically stable solutions ensuring an average Y+ higher than 20, as typically suggested for k-ε turbulence model calculations. Moreover, the default medium quality mesh has been adopted to avoid a huge number of elements and inflation layers technique has not been used, its effect on the overall pressure drop prediction being negligible. Details of meshes selected for SB #08 and #14 are reported in Figures 4 and 5.

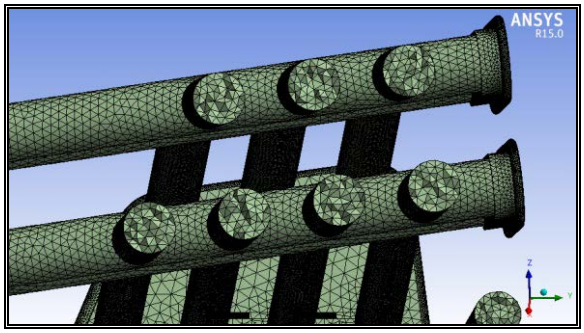

Fig. 4. Detail of mesh selected for SB#08.

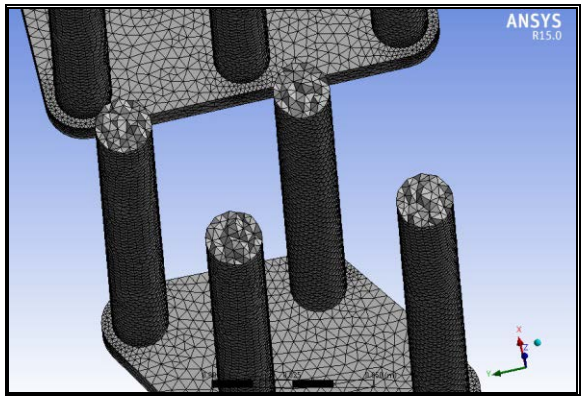

Fig. 5. Detail of mesh selected for SB#14.

The main parameters of finite volume models set-up (Table 1) indicate that the SB #08 finite volume model is much more complex than that of SB #14, therefore requesting much longer calculation times.

Table 1. Summary of mesh parameters.

Mesh parameters	SB#08	SB#14
Nodes	3 485 562	1 133 866
Elements	16 320 217	5 408 654
Avg. Element Quality	0.832	0.834
Avg. Aspect Ratio	1.872	1.865
Avg. Skewness	0.236	0.233

3.3.2 Flow constitutive model

Water thermofluid-dynamic properties defined in the IAPWS IF97 library [7], already implemented in the code, have been adopted to simulate the coolant constitutive behaviour.

3.3.3 Loads and boundary conditions

A proper set of loads and boundary conditions (BCs) has been adopted according to the specific experimental test to be simulated. In particular, the volumetric density of gravity force has been defined within the flow domain, while a proper combination of inlet total pressure and outlet mass flow rate (SB#08) or inlet mass

flow rate and outlet static pressure (SB#14) has been adopted as boundary condition at the flow domain inlet and outlet sections, according to the test specifications. Furthermore, at the interface between the coolant and the circuit steel walls, a no-slip condition has been assumed together with a proper "wall function" algorithm, that allows to effectively model the fluid-wall interaction effects on the overall pressure drop, avoiding the simulation of complex transport processes taking place in the thermofluid-dynamic boundary layer and, consequently, saving calculation time. To this purpose absolute wall roughnesses of 6.3 μm and 10 μm have been assumed for the SB #08 and SB #14 cooling circuits, respectively [6], according to test specifications.

Finally, according to test specifications, isothermal flow at ~293 K has been assumed to reduce the number of equations to be solved and speed-up calculations.

3.3.4 Turbulence model

All the cases investigated are characterized by a turbulent flow pattern. Concerning the turbulence model, the k-ε model has been adopted since it offers a good compromise in terms of accuracy and robustness [4] and is recommended for general purpose simulations. In particular, it uses the scalable wall-function approach that overcomes one of the major drawbacks of the standard wall function use in that they can be applied on arbitrarily fine meshes [5].

3.3.5 Analysis settings

Parametric steady state analyses have been simulated by the ANSYS-CFX code adopting the "false transient" algorithm to speed-up convergence of calculations.

In order to properly set initial values, whose educated guess may contribute to reduce calculation times as well as to the chance that the solution might fail to converge due to diverging residuals [5], an approximate solution, initially obtained using the upwind advection scheme, has been imposed as initial condition to obtain a more accurate final solution. A summary of the main adopted analysis settings is reported in Table 2.

Table 2. Summary of SB#08 CFD analysis settings.

Settings	SB#08	SB#14
Analysis type	steady state	steady state
Water library	IAPWS IF97	IAPWS IF97
Temperature	20 °C	19 °C
Turbulence model	k-ε (C_μ = 0.09)	k-ε (C_μ = 0.09)
Inlet BC	Total pressure	Mass flow rate
Outlet BC	Mass flow rate	Static pressure
Absolute roughness	6.3 μm	10 μm

3.4 Results

Results obtained from the parametric analyses relevant to both SB #08 and SB #14 cooling circuits have been reported in term of hydraulic characteristic functions in Figures 6 and 7 in comparison with the corresponding experimental results. Moreover, the same results are reported in Tables 3 and 4, with the numerical indication of the percentage deviation between numerical predictions and experimental measurements.

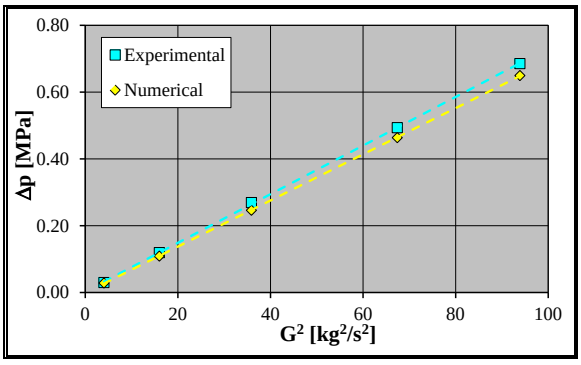

Fig. 6. SB#08 cooling circuit hydraulic characteristic function.

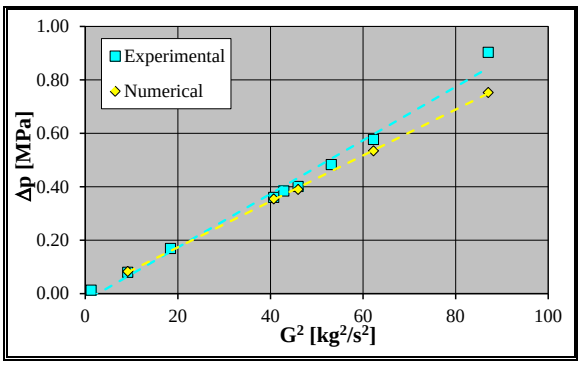

Fig. 7. SB#14 cooling circuit hydraulic characteristic function.

Table 3. Results summary SB#08.

Mass flow rate [kg/s]	Total pressure drop [MPa]		ε%
	Experimental	Numerical	
2.01	0.030	0.028	-4.49%
4.00	0.120	0.109	-8.84%
5.99	0.269	0.246	-8.62%
8.21	0.493	0.463	-6.08%
9.69	0.685	0.649	-5.24%

Table 4. Results summary SB#14.

Mass flow rate [kg/s]	Total pressure drop [MPa]		ε%
	Experimental	Numerical	
1.12	0.013	-	-
3.03	0.080	0.083	3.72%
4.29	0.169	-	-
6.38	0.360	0.354	-1.56%
6.55	0.384	-	-
6.78	0.401	0.390	-2.74%
7.29	0.483	-	-
7.89	0.577	0.534	-7.38%
9.33	0.903	0.753	-16.66%

Numerical predictions show reasonably good agreement with experimental measurements both for SB#08 and SB#14 cooling circuits, but in each case tend to generally underestimate the pressure drop. For the SB#08 cooling circuit, the percentage deviation is lower than 9%, while for the SB#14 cooling circuit the deviation is lower than 10% except for the case corresponding to the highest mass flow rate. In this case a deviation of 16.66% has been calculated, that could be due to an experimental measurement error, as can be deduced by observing, from Fig. 7, that in this case the experimental pressure drop clearly deviates from the assessed trend of proportionality to the square of mass flow rate showing a behaviour different from that observed in SB#08 (Fig. 6).

Pressure and velocity spatial distributions calculated in case of highest mass flow rates both for SB#08 and SB#14 cooling circuits have been reported in Figs. 8-11. Pressure distributions show that the highest pressure drop is concentrated in the central part of both the SB#08 and SB#14 cooling circuits, typically where the highest velocities are attained. In fact, coolant is conveyed in each half of both SB#08 and SB#14 cooling circuits through small feeding pipes where the overall mass flow rate is routed causing high localized pressure drops.

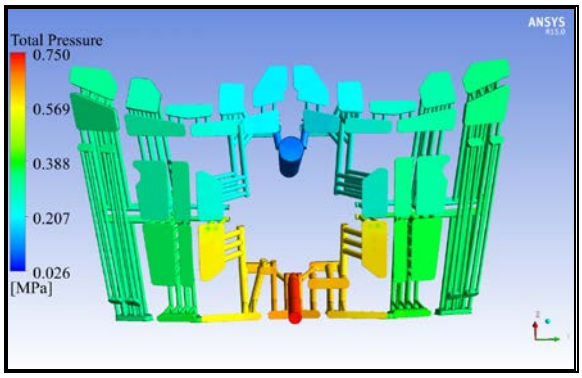

Fig. 8. SB#08 cooling circuit total pressure distribution.

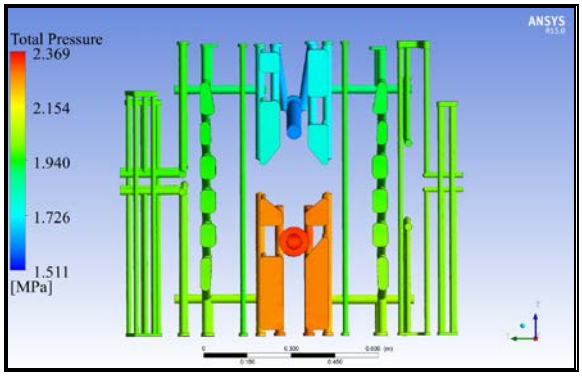

Fig. 9. SB#14 cooling circuit total pressure distribution.

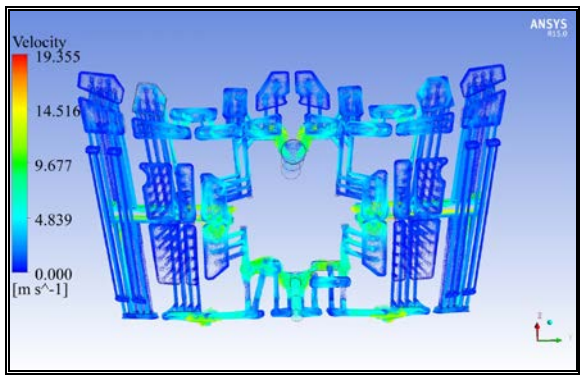

Fig. 10. SB#08 cooling circuit velocity field.

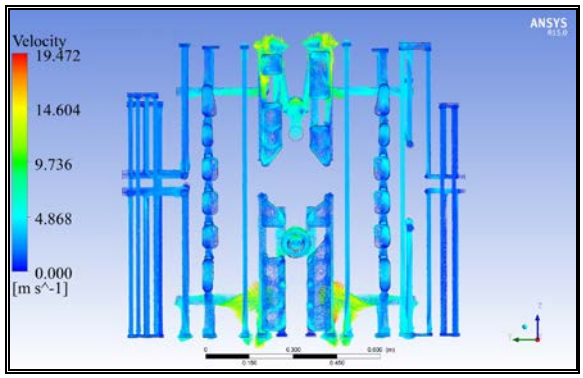

Fig. 11. SB#14 cooling circuit velocity field.

Velocity fields appear to be generally regular (Figs. 10 and 11), moreover, even in the case of highest mass flow rates, the mixing flow velocity along channel networks typically meets the required limit of 7 m/s, related to erosion concerns [8].

4. Conclusions

A theoretical-computational research campaign has been launched to investigate the steady state hydraulic behaviour of SBs #08 and #14 cooling circuits, for which experimental results on full scale prototypes are available and can be compared to numerical simulation results. A CFD approach has been followed and a commercial code has been adopted.

Results obtained have allowed code benchmarking for blanket modules and the numerical predictions have been found to be generally lower than but quite close to the experimental results (with the difference being typically less than 10%). Moreover, calculated pressure and velocity spatial distributions have allowed assessing circuit areas where potential concerns relevant to high flow velocities or localized pressure drop may arise.

Disclaimer

The views and opinions expressed herein do not necessarily reflect those of the ITER Organization.

References

[1] A. R. Raffray, B. Calcagno, P. Chappuis, Zhang Fu, Chen Jiming, D-H. Kim, S. Khomiakov, A. Labusov, A. Martin, M. Merola, R. Mitteau, S. Sadakov, M. Ulrickson, F. Zacchia, The ITER Blanket System Design Challenge, Nuclear Fusion 54 (2014) 033004.

[2] P.A. Di Maio, G. Dell'Orco, A. Furmanek, S. Garitta, M. Merola, R. Mitteau, R. Raffray, G.A. Spagnuolo, E. Vallone, Analysis of the steady state hydraulic behaviour of the ITER blanket cooling system, Fusion Engineering and Design (2015), doi: 10.1016/j.fusengdes.2015.05.070.

[3] P.A. Di Maio, G. Dell'Orco, A. Furmanek, S. Garitta, M. Merola, R. Mitteau, R. Raffray, G.A. Spagnuolo, E. Vallone, Numerical simulation of the transient thermal-hydraulic behaviour of the ITER blanket cooling system under the draining operational procedure, Fusion Engineering and Design (2015), doi: 10.1016/j.fusengdes.2015.01.024.

[4] A. Martin, B. Calcagno, Ph. Chappuis, E. Daly, G. Dellopoulos, A. Furmanek, S. Gicquel, P. Heitzenroeder, Chen Jiming, M. Kalish, D.-H. Kim, S. Khomiakov, A. Labusov, A. Loarte, M. Loughlin, M. Merola, R. Mitteau, E. Polunovski, R. Raffray, S. Sadakov, M. Ulrickson, F. Zacchia, Zhang Fu, Design evolution and integration of the ITER in-vessel components, Fusion Engineering and Design (2015), doi: 10.1016/j.fusengdes.2013.01.004.

[5] ANSYS Inc., ANSYS CFX-Solver Theory Guide.

[6] ITER Organization, personal communications.

[7] International Association for the Properties of Water and Steam, Revised Release on the IAPWS Industrial Formulation 1997 for the Thermodynamic Properties of Water and Steam, Lucerne, Switzerland, 2007.

[8] ITER Organization, internal report.